M. Tech. (Computer Science) Dissertation Series

Tracing the Hot Spots for Placement of Heat Sink in a VLSI Chip Layout

A dissertation submitted in partial fulfillment of the requirements for the M. Tech. (Computer Science) degree of the Indian Statistical Institute

By

Bhaskar Chakraborty

Under the supervision of

Prof. Bhargab B. Bhattacharya

of

Advanced Computing and Microelectronics Unit

INDIAN STATISTICAL INSTITUTE
203, Barrackpore Trunk Road
Calcutta-700108

2004

CERTIFICATE OF APPROVAL

This is to certify the thesis entitled '**Tracing the hot spots for placement of heat sink in a VLSI chip layout**' submitted by Bhaskar Chakraborty towards partial fulfillment of requirements for the degree of M. Tech in Computer Science at Indian Statistical Institute, Kolkata embodies the work done under my supervision.

Dated:

B. B. Bhattacharya
21.7.04

Signed:
(Prof. Bhargab B. Bhattacharya)

Supervisor

Countersigned:

External Examiner

ACKNOWLEDGEMENT

I take this opportunity to express my deep sense of gratitude and indebtedness to my guide Prof. **Bhargab B. Bhattacharya** of Advanced Computing and Microelectronics Unit of Indian Statistical Institute, Kolkata for his generous and wholehearted support to me in doing this project.

I would also like to express my thanks and gratitude to Madam **Sushmita Sur Kolay** of the same unit for her help and guidance to me from time to time during my work and **Mr. Subhasis Majumdar** a former student of Indian Statistical Institute for his help to me in performing various calculations and arriving at the results.

Last but not the least I would like to express my profound gratitude to other research and project fellows of the same unit who helped me in several ways for my work. I would specially thank **Mrs. Suchandra Roy Bagchi** for providing me some of the required softwares during my work.

Bhaskar Chakraborty

Tracing the hot spots for placement of heat sink in a VLSI chip layout

Bhaskar Chakraborty
E-mail: jubhaskar@yahoo.co.in

Abstract

In today's VLSI technology the chip area is shrinking fast in order to meet speed and performance criteria. With the reduction in chip area critical factors like power consumption, power density, and propagation delay come into play. The heat generated due to the power consumption by various elements is radiated through the substrate. Due to reduction in chip size area this accumulated heat may attain very high levels, and consequently the power density may exceed a threshold value at some points on the layout causing thermal damage to the chip. In this dissertation, a geometric approach is presented to model and identify these hot spots. Results based on simulation are also reported.

Index

Contents | Page

Chapter 1

Introduction

1.1 What is a heatsink?

All semiconductor devices have some electrical resistance just like resistors and coils etc. This implies that when power diodes, power transistors, and power MOSFETs are switching or controlling reasonable currents, they dissipate power as heat energy. Now if the device is not to be damaged by this, this heat must be removed from the device at such a rate such that the temperature rise is kept to a certain predefined value. **Heat sinks** are used to do this.

We may consider heat sink as something having a thermal resistance, which behaves in a very similar way to electrical resistance; the more the heat energy flowing through it(analogous to electrical current flowing through it) the higher the temperature rise across it(analogous to voltage drop across it).

In fact, there is a **thermal equivalent** to **Ohm's law**, which shows the way the heat energy behaves in something like a power transistor:

$$\mathbf{T\ (j\text{-}a) = P_d * R_{th}\ (j\text{-}a)}$$

Here T (j-a) is the **temperature rise** of the transistor's heat producing junction, above that of the surrounding environment temperature (roughly air temperature); P_d is the **total power** being dissipated; and R_{th} **(j-a)** is the **total thermal resistance** between the junction and the surrounding environment. Fig 1.1 shows this explicitly.

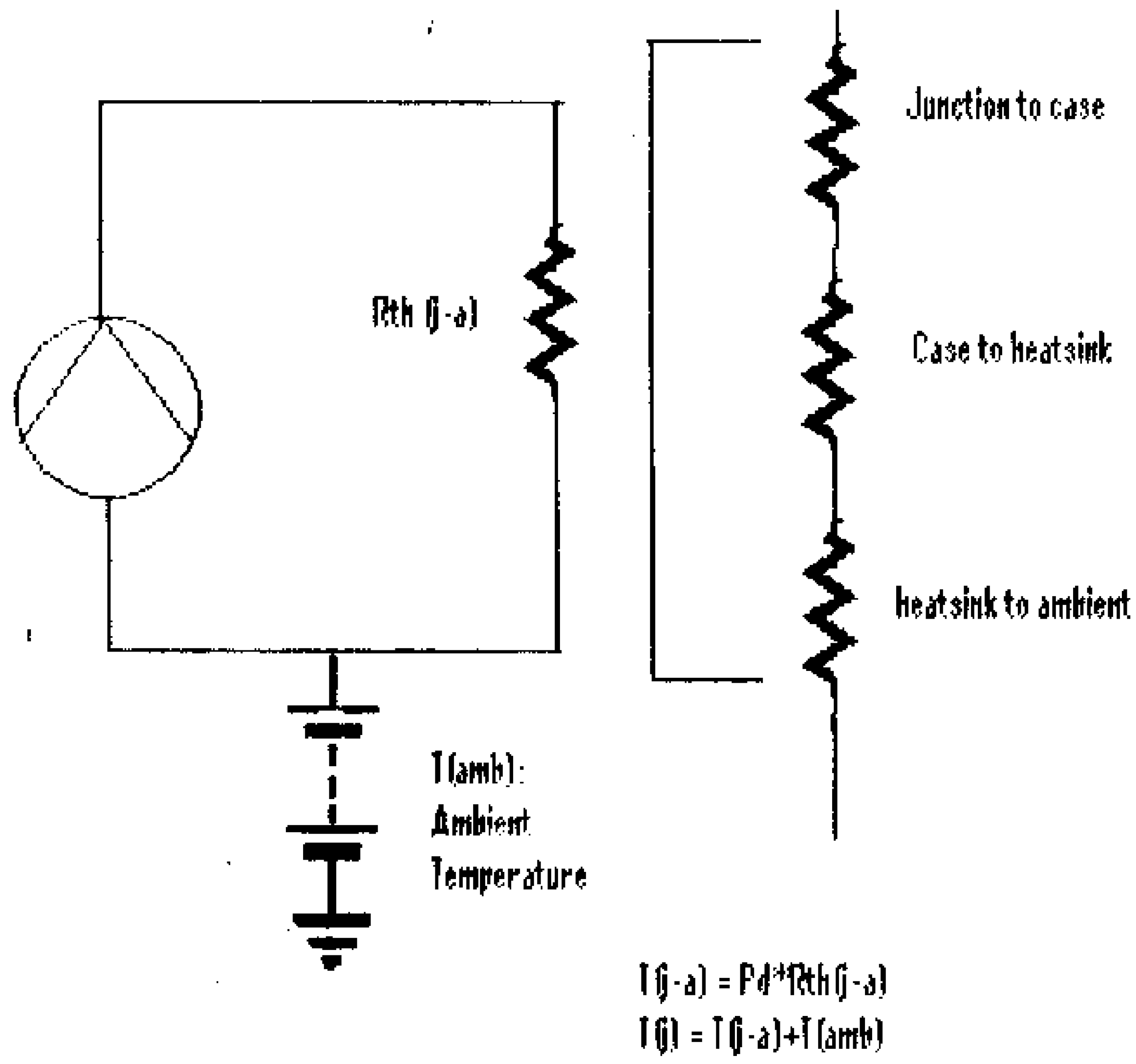

Fig 1.1 Heat sink as a combination of resistances in series.

T (j-a) is normally measured in degree Celsius, P_d in watts and R_{th} in degree Celsius/watt.

So if we want to keep the temperature rise in the transistor below a safe level for a given finite power dissipation and for a given ambient temperature, we can do it only by reducing the value R_{th} (j-a). Now R_{th} (j-a) is really made of two thermal resistances in series viz. the resistance in the device package between the junction and its outside case called R_{th} (j-c) and the other is between the case and the ambient, R_{th} (c-a). Now very little can be done to control the value of R_{th} (j-c) but fortunately its value is low (between 0.7 to 4.5 degree Celsius per watt. But we can certainly do something about R_{th} (c-a) and here is where the use of heat sink comes in.
Now if a power transistor or MOSFET package is simply supported by its lead above a PC board and surrounded by air, heat energy can mainly flow from the case to the ambient either by air convection or by radiation. As a result the thermal resistance to ambient R_{th} (c-a) is fairly high – typically between 35 and 100 degree Celsius per watt.

1.2 Hot spots in VLSI chip

In a VLSI chip there are millions of active elements (transistors) and other regions, which during operation generate heat. Heat generated from all these points add up through out the chip. At some point(s) inside the chip the net heat received from all these heat-generating elements may become quite high and surpass a predefined safe limit. So to control the unnecessary increase in power and the consequent temperature rise suitable heatsinks should be designed considering this (these) critical point(s), called hot spot(s)..

Chapter 2

Determination of Hot spots: Proposed Models

2.1 The continuous unit circle model

In this model we assume a continuous domain for the chip under consideration. We calculate the total power received at any point in the chip by calculating the power received from each active heat-generating source at that point by the formula derived in this model and then summing them up. We assume that the heat-generating sources are placed randomly throughout the chip. The model is described below:

The unit circle model is shown in Fig 2.1 .We assume that a heat-generating source S with power P is placed at a point (a, b) in the chip. Next we assume that our point of consideration t is placed at point (p, q) in the chip. Let d be the distance from source S to target t.

Consider a circle with unit radius around center t and also an imaginary circle with radius d around center S. As shown in the figure the angle subtended at the center S by the arc of the imaginary circle that is present inside the unit circle is 2θ. So the fractional contribution of S at t is going to be $2Pd\theta/2\pi d = \theta/\pi$. Using simple geometry we can derive that $\sin(\theta/2) = 1/(2d)$. Hence we can write θ as 2*Arcsine (1/2d). So given the Euclidean distance d and power P of an active source S from a target we can use the formula

P_r = 2*P* Arcsine (1/2d) / π

to calculate its fractional heat contribution P_r at the target point.

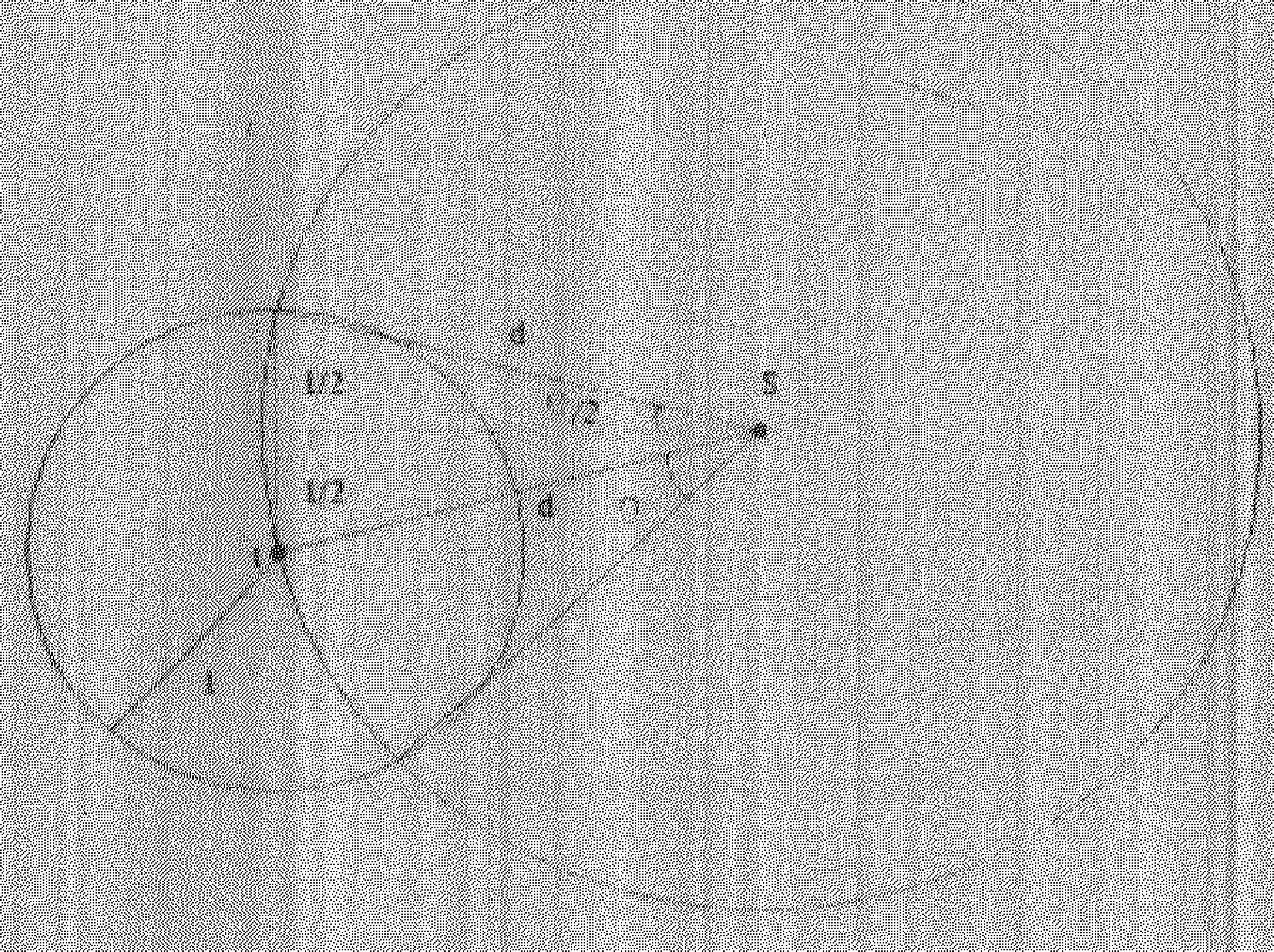

Fig 2.1. The unit circle model

In this project we address the problem of determining the location of hottest points on the chip floor. Intuitively, the active source points definitely belong to the above class. But the more important question is whether the active sources are the only points that need be considered. We will rather put the question in a different way. Are there any non-source points on the floor that are hotter than any of the active source points? Our observation is that the answer to the above question may be **yes** and it is not difficult to find out such examples.

It is easier to locate such examples when the strengths of the heat sources vary over a wide range. Using **Mathematica** (an engineering software developed by Wolfram Research Organization, UK) we show that even for test cases with a very few sources with same strength, such points exist. Before we proceed further, we want to mention two special cases of the unit circle model. In Fig 2, we first consider case I where the source S lies quite close to the target point t such that it comes inside the unit circle around t. Here the distance d between S and t is less than 1 but more than 1/2. The angle 2θ subtended at S is greater than $2\pi/3$ and consequently more than 1/3 of the power emanating from S reaches the unit circle around t. In case II, S comes further close to t such that the distance d is less than 1/2. So the circle with radius d around S now lies entirely within the unit circle around t. This implies that the entire heat coming out of S reaches the unit circle in this case.

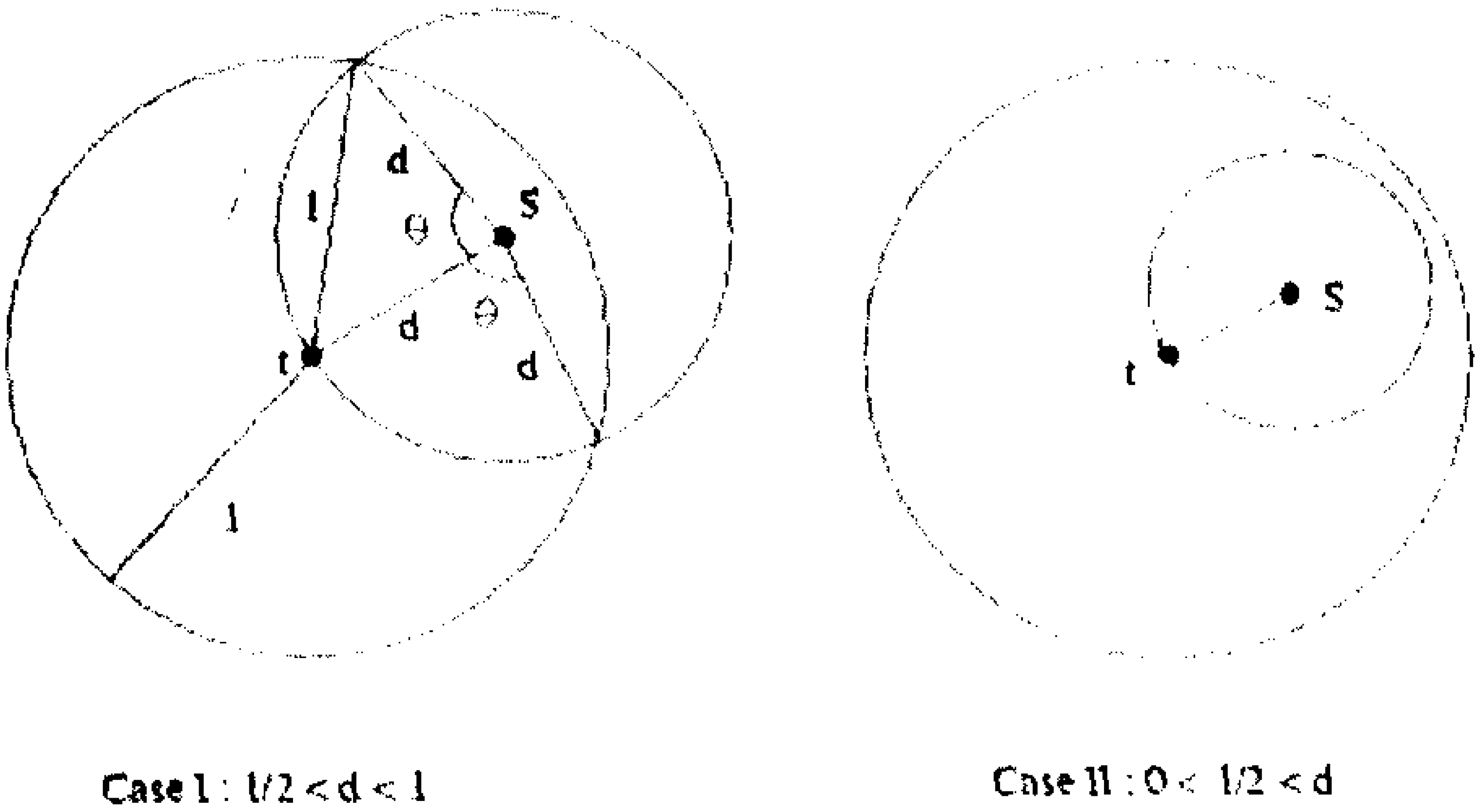

Fig 2.2 Special cases for the unit circle model

2.2 The discrete grid model

The model, which we have discussed, previously assumes a continuous domain. It's normally more tedious and cumbersome to perform calculations and arrive at results in the continuous domain. We can however consider another domain for our convenience, which considers the layout to be a grid based one and the source points are placed only at a finite number of discrete points on the grid. The propagation of heat energy assumed in this model is as discussed below:

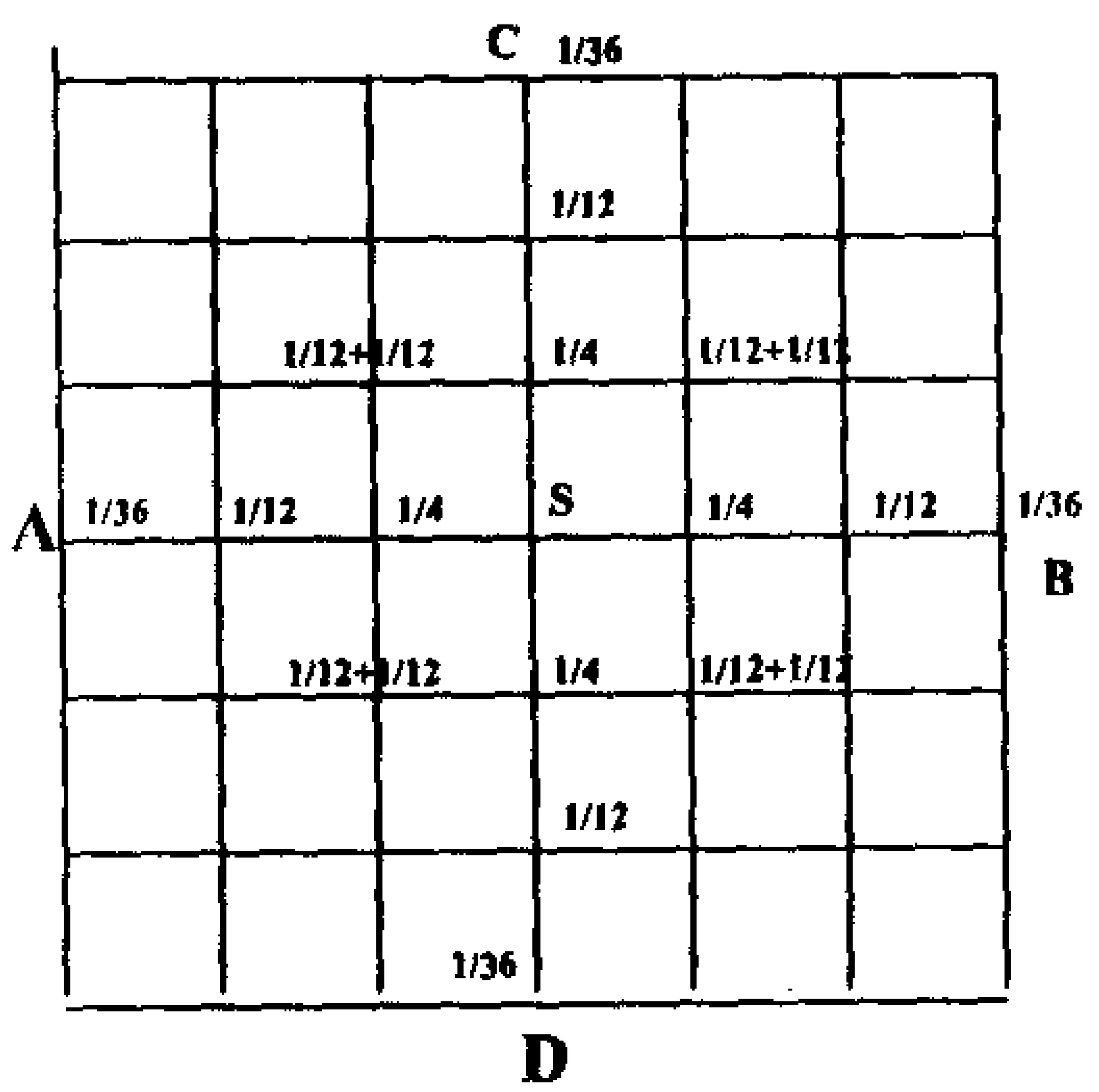

Fig 2.3. 6 x 6 grid with source at [4,4]. Note the propagation of power around the source

In Fig 3 is shown a source S placed in a chip, which is divided into a grid of size 6 by 6. The source sends ¼ th of its power to its four nearest neighbors as shown. Each of these 4 neighbors transmits 1/3rd of its received power to three of its nearest neighbors away from the source as shown.

From hereon all the points which lie on lines AB and CD which contain the source transmit 1/3rd of their received power to their neighboring grid points away from the source. Those, which lie on the boundary, transmit half of their received power to their nearest neighbors as shown below. If however a corner point is reached the power retransmission stops there. Points that don't lie either on AB or CD transmit half of their received power to two of their neighboring grid points in a direction away from the source. We define the power propagation factor of a grid point or simply its propagation factor to be the fraction of the power it receives from a given source. The grid points may be divided into several frontiers w.r.t the source. It can be shown that the sum of the propagation factors of all grid points in a particular frontier is equal to 1. This has been shown in Fig 4.

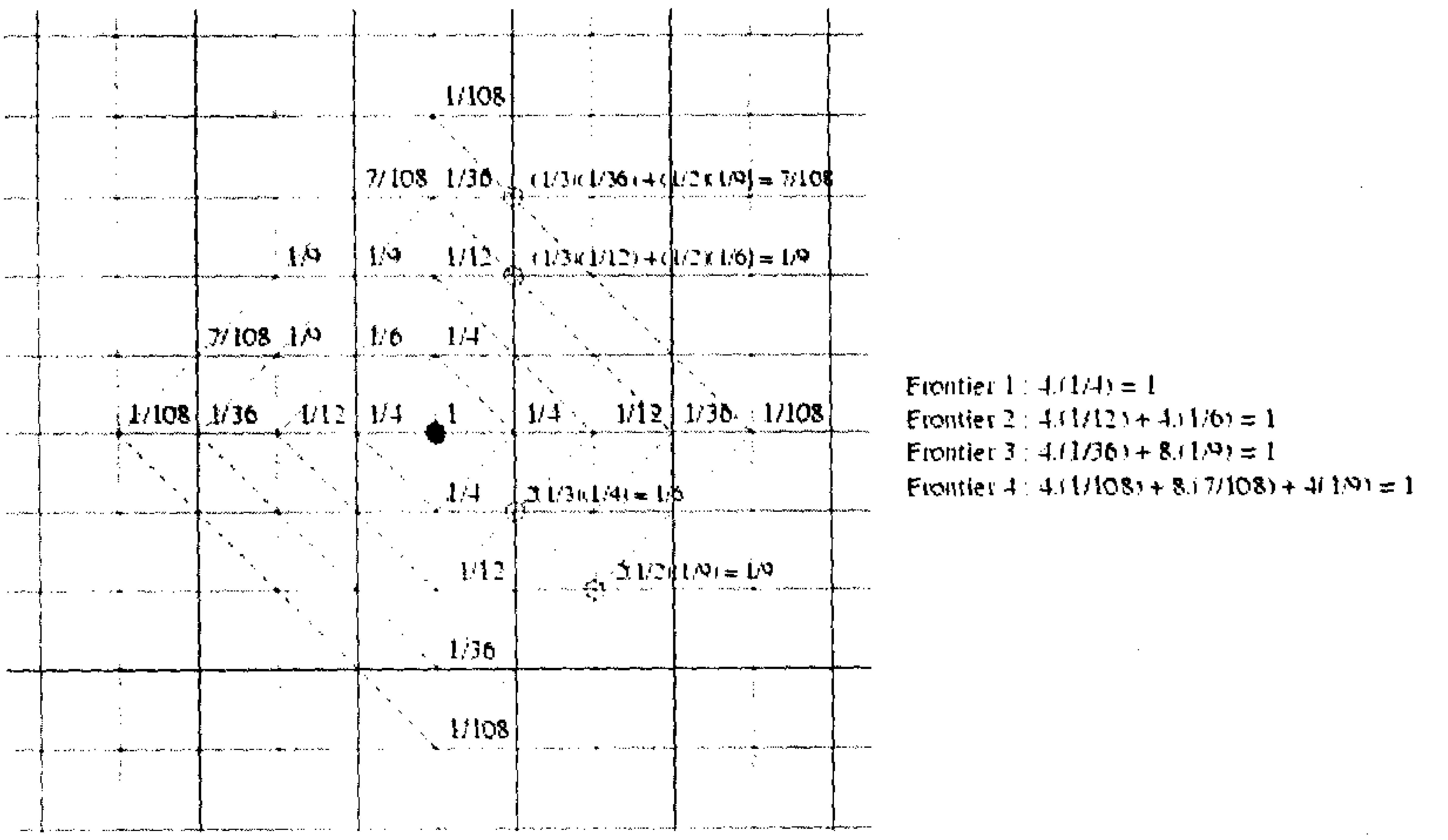

Fig 2.4. The frontiers are shown above as dotted squares. Note that the sum of power propagation factor along each frontier is 1

For points that lie either on the horizontal or vertical line passing through the source the propagation factor is given by

$$P_f\,[x, s_2] = 1/(4*3^{|x-s_1|-1}), \qquad \text{for } |x-s_1| > 0$$
$$P_f\,[s_1, y] = 1/(4*3^{|y-s_2|-1}) \qquad \text{for } |y-s_2| > 0$$

where $[s_1, s_2]$ is the source under consideration and $[x, s_2]$ is any point on the horizontal line passing through the source and $[s_1, y]$ is any point on the vertical line passing through the source.

For points that lie either on the horizontal or vertical line which are at a unit grid distance from the horizontal or vertical lines containing the source the propagation factor is given by

$$P_f\,[x, s_2 \pm 1] = 1/(3*2^{|x-s_1|-1}) - 1/(2*3^{|x-s_1|}) \qquad \text{for } |x-s_1| > 0$$
$$P_f\,[s_1 \pm 1, y] = 1/(3*2^{|y-s_2|-1}) - 1/(2*3^{|y-s_2|}) \qquad \text{for } |y-s_2| > 0$$

For points other than those considered in the above two cases the propagation factor is given by

$$P_f\,[x, y] = (½)*[\{ \sum_{k=2}^{x} [1/(3*2^{k-1}) - 1/2*3^{k}] \; * \; {}^{x+y-(k+2)}C_{x-k} \; * \; (½)^{x+y-(k+2)}\} \; +$$
$$\{ \sum_{k=2}^{y} [1/(3*2^{k-1}) - 1/(2*3^{k})] \; * \; {}^{x+y-(k+2)}C_{y-k} \; * \; (½)^{x+y-(k+2)}\}] \,.$$

Please refer to Appendix A for the derivation of these results.

Chapter 3

Observations and Results

3.1 The continuous unit circle model

In the continuous model we obtained results for the special case of a regular polygon containing sources at each of its vertices with all or some of the sources being active. Next, we studied the behavior for a random placement of sources in the chip using the Monte Carlo approach. In the continuous unit circle model all the calculations have been done according to the assumptions and the formula derived for that model previously.

3.1.1 Regular polygon analysis

For the case of the regular polygon initially we assume that the sources are present at the vertices of a regular polygon of n sides with all the sources having equal power. In that case we came up with the following observations.

Let n be the number of the sides of the polygon and r be the distance from its center to any of the vertices in some unit. Assume that initially identical power P_s = 1 mw to each of the source present at the vertices. Table 1 shows the net power induced at the source due to presence of other sources and also the maximum power inside the regular polygon for various values of n and r.

n	r	P_s(induced)	P_{center}	$P_{max\text{-}inside}$	d*
4	5	1.12195	0.255074	1.12825	4.5
4	10	1.06094	0.127377	1.06249	9.5
4	15	1.04062	0.084898	1.04131	14.5
8	5	1.35773	0.510148	1.37506	4.5
8	10	1.17864	0.254754	1.18304	9.5
8	15	1.11906	0.169797	1.12103	14.5
4	50	1.01354	0.0254652	1.01225	49.5
8	50	1.03968	0.0509304	1.03589	49.5
4	100	1.00609	0.0127324	1.00611	99.5
8	100	1.01786	0.02546	1.0179	99.5
4	200	1.00305	0.0063662	1.00305	199.5
8	200	1.00893	0.0127324	1.00894	199.5
4	500	1.00122	0.002546	1.00122	499.5
8	500	1.00357	0.005093	1.00357	499.5
20	500	1.01265	0.0127324	1.01266	499.5
50	500	1.04091	0.031831	1.04093	499.5

Table 1 The above table shows the power values for different combinations of r and n.

* d here stands for the distance from center to the maximum point which lies along the line from the center to a source

From the above table we find that when n and r are both small then the value of $P_{max\text{-}inside}$ slightly exceeds the power induced at the source. However, the maximum value occurs at the edge of the unit half-circle about any of the source. As the value of n and r increases the value of $P_{max\text{-}inside}$ approaches the value of P_s (induced) of the source. So the slight difference in $P_{max\text{-}inside}$ is due to our assumptions of the model that inside the unit half circle about the source the received power will be the same as generated by the source.

Hence, in all these cases the value of the induced source power is more than that at any other point inside the polygon. The plot in Fig 3.1 shows the variation of power for n = 8, and r = 50.

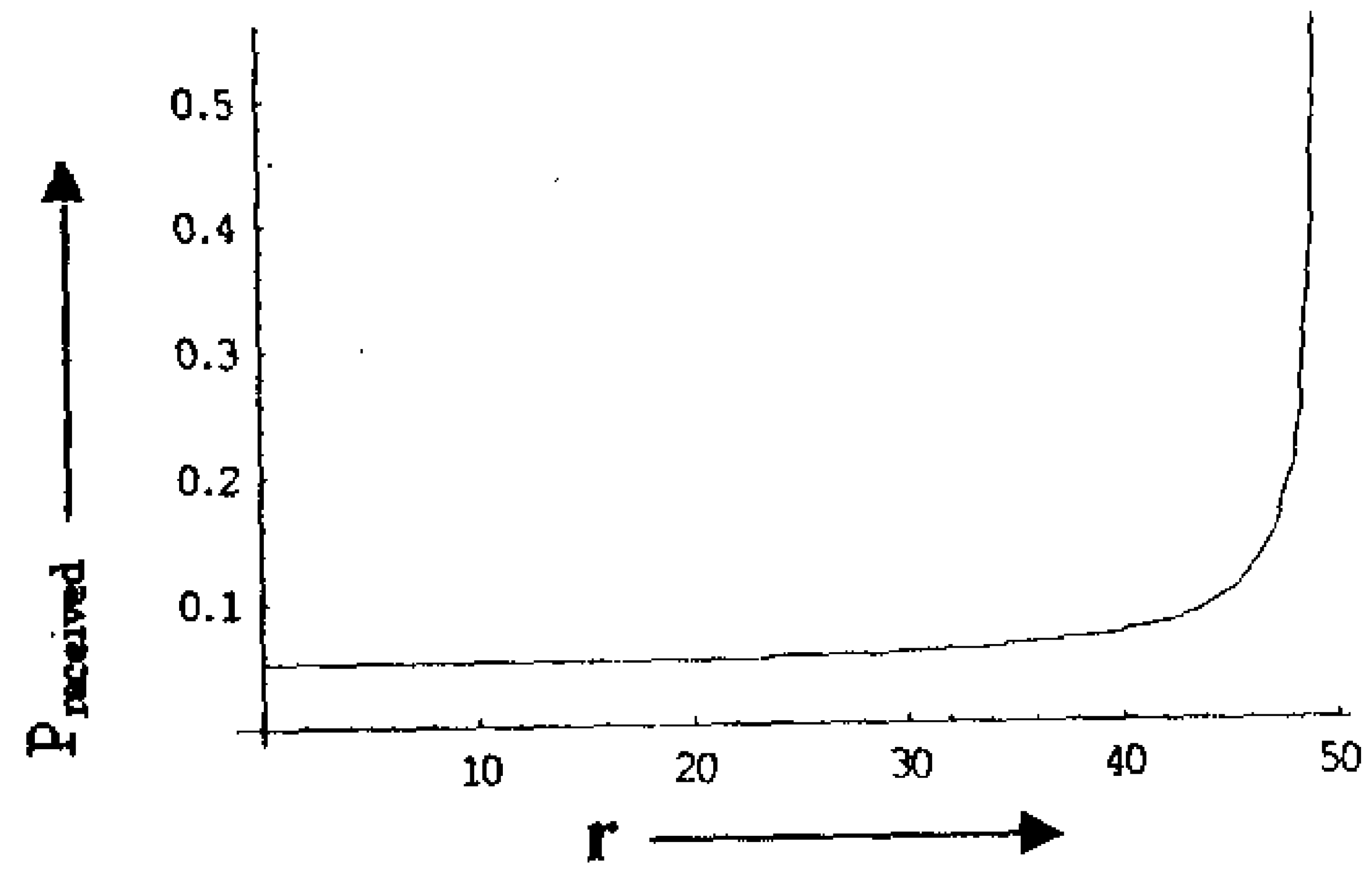

Fig 3.1. Plot showing the variation of net received power against the distance from the center to the source along the line from center to the source

In the above observation the initial source powers had been taken to be the same. If however we give different values to the sources then a point or more than one point inside the polygon may receive power exceeding the minimum of the source-induced powers. This is proved by the following observation.

Take n = 4, r = 5, $P_s[1] = 1.2$, $P_s[2] = 5.2$, $P_s[3] = 37.8$, $P_s[4] = 5.2$ each power being in milliwatts we have the induced power at the source-1 = 2.87227 mw, while induced power at the center = 3.15017 mw.
So the induced power at the center **exceeds** that at source-1.

So what we want to establish from the above discussion is that there may be points or regions on the floor, which **do not contain any active source point** but they are **hotter** than some of the active source points. So it may not be enough to just guard the active source points in order save a chip from getting burnt.

3.1.2 Monte-Carlo analysis for the unit-circle model

In doing Monte-Carlo analysis we consider a chip layout with some sources selected randomly on it. Then we select some random points in the layout, and some other points selected very near to the sources deliberately (since the effect of the source is more pronounced near it). Next we study the power received in these chosen points as well as at each of the sources. A **threshold** is chosen which we have taken to be the **minimum** of the **induced power** among all the **sources.**

Let n denote the number of sources chosen randomly in the layout. Let the layout be of size 600 x 600. We are choosing **two sets of points** at which we calculate and study the net power received from all the sources. In one set we consider those points that **are very near** to the one of the randomly generated sources while in another set we consider those points which **are generated entirely randomly** and are present anywhere in the layout. The reason for choosing the former set of points is that we have observed that in the unit circle model in a continuous domain points which are very near to the source receive very high power compared to those which are at moderate or large distance away from the source. So for each source we consider a hypothetical square, which contains that source at its center. We divide that square into a hypothetical grid with a particular size and include each of the produced grid points as our points of study for the first set of points as we have described earlier. All these points generated constitute the first set of points. The second sets of points are generated entirely randomly.

With these assumptions we have recorded the following observations using the assumptions and formulae of the unit circle model for continuous domain. The hypothetical square around each source has been taken to be of size 10x10, which is divided into a hypothetical 20x20 grid containing 400 points that are present very near to the source. The records have been tabulated in table 2. In this experiment we have assumed the sources to be at fixed locations and have constant generating power in each trial for a particular number of sources. Their locations and generating power have been determined randomly at the beginning of the 1st trial, the generating power being randomly selected between 1 and 25 mw. It's only the testing points which lie in the second set of points as defined earlier that are varied at each trial. The probe points column given in table 2 consists of points from both the sets.

Trial	n	Threshold	# probe pts	# pts. above threshold	P_1*	P_2*
1	5	9,53	4500	73	68	0
2	5	9.53	4500	73	68	0
3	5	9.53	4500	73	68	0
4	5	9.53	4500	73	68	0
5	5	9.53	4500	73	68	0
1	10	7.48	14000	166	156	0
2	10	7.48	14000	167	157	1
3	10	7.48	14000	170	160	2
4	10	7.48	14000	166	156	0
5	10	7.48	14000	167	1157	0
1	20	8.67	30500	844	824	13
2	20	8.67	30500	856	836	18
3	20	8.67	30500	842	822	12
4	20	8.67	30500	847	827	15
5	20	8.67	30500	848	828	15
1	40	9.95	56000	1706	1666	30
2	40	9.95	56000	1714	1674	38
3	40	9.95	56000	1708	1668	31
4	40	9.95	56000	1725	1685	42
5	40	9.95	56000	1711	1679	38
1	50	10.82	60000	1902	1852	43
2	50	10.82	60000	1911	1861	47
3	50	10.82	60000	1931	1881	49
4	50	10.82	60000	1937	1887	50
5	50	10.82	60000	1924	1874	42

Table 2

*** P_1 is the # of non-source points that have the received power above or equal to the threshold value while P_2 is the # of non-source points which lie outside the source boundary considered that have the received power above or equal to the threshold value.**

Fig 3.2 shows the plot for trial 2 for n = 10 in the next page.

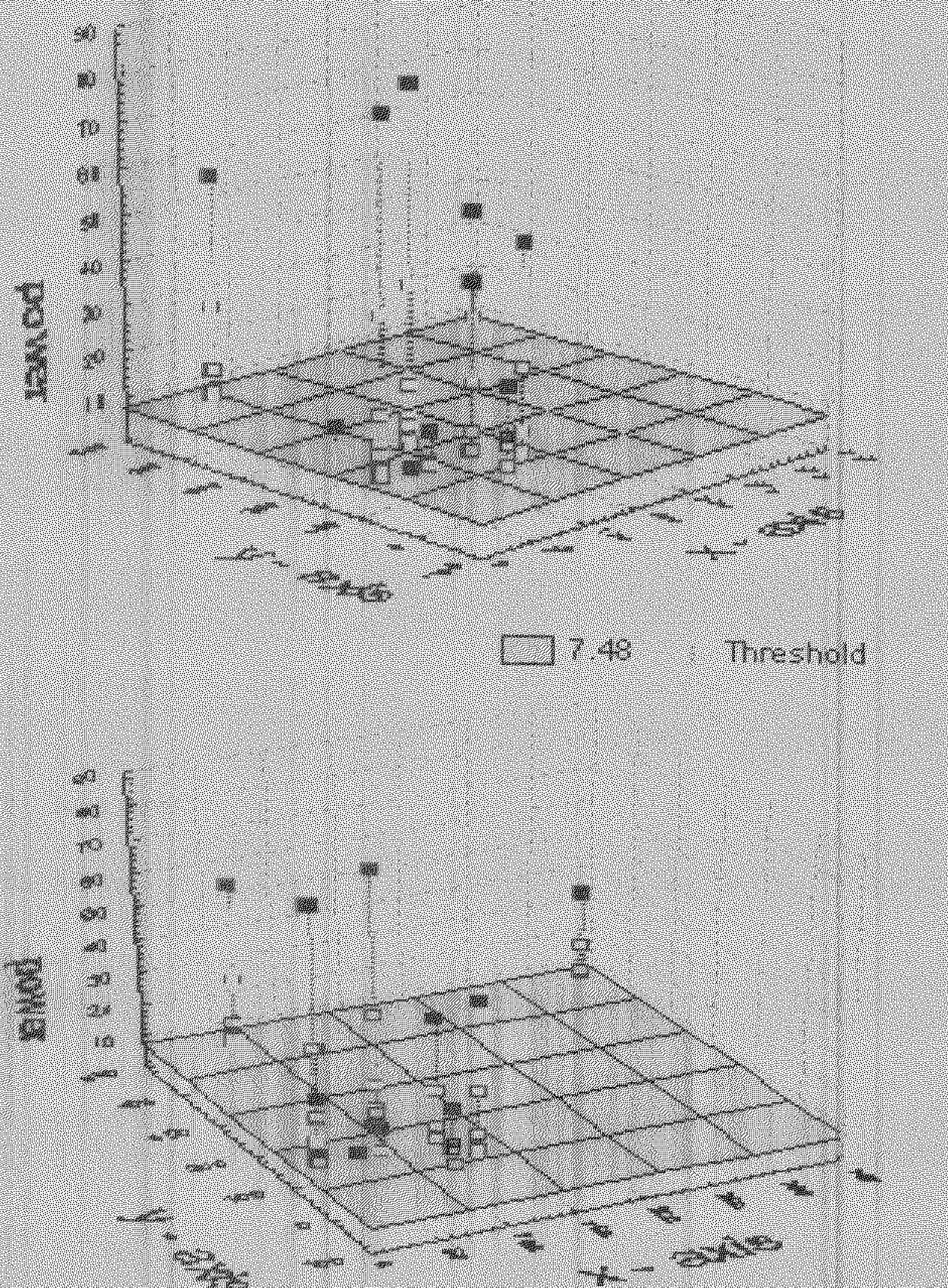

Fig 3.2: 2 views of the points crossing threshold are shown for trial 2 with 10 sources as tabulated in table 2. The sources are shown by a filled marked red rectangle at the top. The bunch of points that belong to the 1st set of points considered and who's received power crosses the threshold are shown by sets of green rectangles at their top. The point P shown is the only non-source point which lies in the second set of points considered that crosses the threshold.

In table 3 we have recorded the observations for a **varying threshold** keeping the source points and their generated power to be fixed. The experiment was done for trial 2 with 20 sources as shown in **table** 2. The threshold is **varied** by a **fixed amount** from the minimum induced source power 8.67 mw to the maximum of the original source powers in this trial, which is 18.4 mw. We observe that the number of points in both the sets P_1 and P_2 decreases rapidly with increasing threshold and at one point it becomes zero.

Trial	n	Threshold	# probe pts	# pts. above threshold	P_1	P_2
1	20	8.67	30500	856	836	18
2	20	10.6	30500	214	194	7
3	20	12.55	30500	78	58	1
4	20	14.5	30500	22	2	0
5	20	16.45	30500	6	0	0
6	20	18.4	30500	0	0	0

Table 3

3.2 The grid based discrete model

3.2.1 Monte-Carlo analysis for the grid based model

We can do the Monte-Carlo analysis for the grid-based model as well in a similar fashion as we did for the continuous model.
In the grid based model we assume a finite number of sources distributed randomly in the grid and we study the power propagation effects among all the grid points.

We recorded the following observations using the assumptions and formulae of the grid based model for discrete domain. A 50 x 50 grid with each side of grid length 50 has been considered. The records have been tabulated in table 4. In each trial the power of each source has kept fixed while their position is varied randomly. The threshold value is the minimum of the induced power of the sources.

Trial	n	Threshold	# probe pts	# pts above threshold	# non source pts above threshold
1	5	3.405	2601	12	7
2	5	3.405	2601	12	7
3	5	5.212	2601	8	3
4	5	4.931	2601	8	3
5	5	3.93	2601	9	3
1	10	6.044	2601	17	7
2	10	4.76	2601	72	62
3	10	4.08	2601	120	110
4	10	6.365	2601	21	11
5	10	3.80	2601	167	157
1	20	7.55	2601	66	46
2	20	6.40	2601	184	164
3	20	6.65	2601	132	112
4	20	6.88	2601	112	92
5	20	7.30	2601	87	67
1	40	9.81	2601	523	483
2	40	10.78	2601	329	289
3	40	10.32	2601	404	364
4	40	9.35	2601	507	467
5	40	9.92	2601	489	449
1	50	12.34	2601	357	307
2	50	12.39	2601	551	501
3	50	9.11	2601	442	392
4	50	9.64	2601	656	606
5	50	10.3	2601	752	702

Table 4 This table shows the number of grid points, which exceed the threshold value for different number of sources. For any number of sources five trials have been done. Before the start of trial 1 the source powers are fixed after choosing them randomly between 1 and 50 mw and subsequently their positions are varied randomly at each trial. The number of non-source points, which exceed the threshold, is also shown.

In table 5 we have recorded the observations for a **varying threshold** keeping the source points and their generated power to be fixed. The experiment was done for trial 3 with 20 sources as shown in table 4. The threshold is **varied** by a **fixed amount** from the minimum induced source power 6.65 mw to the maximum of the original source powers in this trial, which is 20.2 mw. We observe that the number of grid points which have received power crossing threshold decreases rapidly with increasing threshold and at one point the number of such non-source points becomes zero.

Trial	n	P^*_{th}	# probe pts	# pts above P_{th}	# non source pts above P_{th}
1	20	6.65	2601	132	112
2	20	9.35	2601	68	24
3	20	12.05	2601	16	3
4	20	14.75	2601	6	0
5	20	17.45	2601	4	0
6	20	20.2	2601	1	0

Table 5

*P_{th} stands for the threshold value considered.

3.2.2 Window based approach

In this approach we are given a fixed size window and a given threshold P_{window} and we are to find out whether there exists a rectangular window in the grid which has the given size and whether the sum of the received power at all points inside it including at its boundary reaches or exceeds P_{window}. If it exists then we need to record the positions of all such windows in the grid layout.

For a 50 x 50 grid the following observations have been recorded for size varying windows using the assumptions and formulae of the grid based model. The observations are shown in Table 6. P_{window} considered here is the product of the minimum induced source power times the number of grid points inside the window i.e.

$P_{window} = (s+1) * (s+1) * P_{th}$ where P_{th} is the minimum induced source power and s is the side length of the window.

Trial	n	s	P_{th}	P_{window}	n_1^*	n_2^*
1	5	3	8.104	129.665	0	0
2	5	3	7.79	124.61	0	0
3	5	5	7.285	262.28	0	0
4	5	5	7.26	261.38	0	0
1	10	3	6.41	102.515	26	0
2	10	3	4.025	64.40	101	19
3	10	5	4.57	164.36	26	0
4	10	5	8.374	301.46	0	0
1	20	3	6.73	1.7.67	57	0
2	20	3	6.66	106.575	82	2
3	20	5	6.135	220.87	18	0
4	20	5	6.67	240.22	11	0
1	40	3	9.58	153.26	136	12
2	40	3	8.32	133.13	378	139
3	40	5	9.82	353.43	187	20
4	40	5	10.03	361.21	0	0
5	40	5	6.77	243.75	854	243

Table 6

* Here n_1 stands for the number of windows that cross the threshold value while n_2 is the number of windows among n_1 that don't contain any source.

Continuing with trial 5 in table 6 we studied the effect of **increasing** the **threshold value** from P_{th} which is the minimum induced source power to P_{max} which is the maximum initial source power before the effect of other sources are considered keeping the source locations and values to be fixed. The maximum initial source power in this case is 20.2 mw. P_{th} is varied from 6.77 to 20.2 mw in 6 trials and the values of n_1 and n_2 are noted. These observations have been recorded in table 7. We observe that the number of windows which have net accumulated power crossing threshold **decreases rapidly** with increasing threshold and at one point the number of such windows which don't contain any source point becomes zero.

Trial	n	s	P_{th}	P_{window}	n_1	n_2
1	40	5	6.77	243.75	854	243
2	40	5	9.00	324	299	37
3	40	5	11.23	404.28	76	2
4	40	5	13.46	484.56	11	0
5	40	5	15.69	564.84	4	0
6	10	5	17.92	645.12	1	0

Table 7

Chapter 4
Conclusion

4.1 Conclusion and Suggestions for future work

We have used Mathematica for doing all the experiments we have done. We have proposed a number of models both in the continuous and discrete domain to model the thermal behavior of a VLSI chip. One important aspect we have observed in all the models is that there are regions in the chip which may become substantially hot even without containing any active heat source. We conclude that it may not be enough to guard only the active regions to make the chip thermally safe. In this dissertation we have mainly presented simulation based results. Future work may be done on finding **efficient geometry-based algorithms** to make the search efficient in the discrete domain, i.e., a methodology can be designed so that the thermal pattern of the chip may be predicted correctly without probing all the grid points. In this dissertation we didn't consider any **time varying sources** i.e. sources which transmit different power in different times. Such sources may also become inactive at some point of time. So a detailed work on the generalized model having time-varying sources can be done. Finally when a set of points on the floor is reported to be hotter than the permissible value by the above method, work can be done on **dilating** the source points using a **Voronoi-based scheme** so that the chip can operate at a safe temperature.

4.2 Bibliography

Tsai2000 C. H. Tsai and S. M. Kang, "Cell-Level Placement for Improving Substrate Thermal Distribution", {\it IEEE Transactions on CAD of Integrated Circuits and Systems}, pp. 253-265, 2000.

Cheng1999 Y. K. Cheng and S. M. Kang, "An Efficient Method for Hot-spot Identification in ULSI Circuits", {\it Proc. of IEEE Int. Conf. on Computer-Aided Design (ICCAD)}, 1999.

Kang2002 S. M. Kang, "On-chip Thermal Engineering for Peta-scale Integration", {\it ISPD}, pp. 76, 2002.

Chu1997 C. N. Chu and D.F. Wong, "A Matrix Synthesis Approach to Thermal Placement", {\it Proc. of Int. Symp. on Physical Design}, pp. 163-168, 1997.

Appendix

Calculation of power propagation factor for the grid-based model

For the grid-based model we calculate separately the propagation factor for grid points lying on the horizontal and vertical lines passing through the source, for grid points lying on horizontal and vertical lines parallel to and a single grid distance away from the above lines and lastly for all the remaining points in the layout. We consider each of these situations separately in three cases below.

Case I

Consider a grid of size a X b with a being the grid length along the horizontal direction and b being the grid length along the vertical direction. Let the bottom left corner grid point be represented by the point [0, 0] and the top right corner by the point [a, b]. Consider a source present at point $[s_1, s_2]$.

Now for all grid points lying either in the vertical line or in the horizontal line passing through the source we have the following simple recurrence relation which follows directly from the power propagation assumptions (refer page 5) we have made for the grid-based model.

$P_f[x, s_2]=P_f[x-1, s_2]*1/3$ for $x > s_1 +1$ ....(1.1)
$P_f[x-1, s_2]=P_f[x, s_2]*1/3$ for $x < s_1$ ....(1.2)
$P_f[s_1, y]=P_f[s_1, y-1]*1/3$ for $y > s_2 +1$ ....(1.3)
$P_f[s_1, y-1]=P_f[s_1, y]*1/3$ for $y < s_2$ ....(1.4)

with $P_f[s_1+1, s_2]= P_f[s_1-1, s_2]= P_f[s_1, s_2+1]= P_f[s_1, s_2-1]=1/4$

where $P_f[x, y]$ is the propagation factor for the point [x, y] with respect to the source under consideration.

Solving relation (1.1) to (1.4) we get the power propagation factor for a grid point lying either on the horizontal line or on the vertical line each of which contains the source as given by

$P_f[x, s_2]= 1/(4*3^{|x-s_1|-1})$. ....(1.5)
$P_f[s_1, y]= 1/(4*3^{|y-s_2|-1})$. ....(1.6)

Case II

Consider next the grid points lying on vertical or horizontal lines at unit grid distance from the lines passing through the source.

For all points lying on the horizontal or vertical lines parallel to the above lines considered above and at a single grid distance from them we proceed as follows. Without loss of generality we consider one such point lying on the horizontal grid line passing through the source. Then according to our assumptions for the propagation pattern in the grid-based model we have the following recurrence relation for the given source at $[s_1, s_2]$.

$$P_f[x, s_2 \pm 1] = P_f[x-1, s_2 \pm 1] * \tfrac{1}{2} + P_f[x, s_2] * 1/3 \quad \text{for } x > s_1 \quad \ldots\ldots\ldots\ldots(2.1)$$
$$P_f[x, s_2 \pm 1] = P_f[x+1, s_2 \pm 1] * \tfrac{1}{2} + P_f[x, s_2] * 1/3 \quad \text{for } x < s_1 \quad \ldots\ldots\ldots\ldots(2.2)$$
$$P_f[s_1 \pm 1, y] = P_f[s_1 \pm 1, y-1] * \tfrac{1}{2} + P_f[s_1, y] * 1/3 \quad \text{for } y > s_2 \quad \ldots\ldots\ldots\ldots(2.3)$$
$$P_f[s_1 \pm 1, y] = P_f[s_1 \pm 1, y+1] * \tfrac{1}{2} + P_f[s_1, y] * 1/3 \quad \text{for } y < s_2 \quad \ldots\ldots\ldots\ldots(2.4)$$

Now substituting the values obtained from case I for $P_f[x, s_2]$ and $P_f[s_1, y]$ in the above relations (2.1) to (2.4) and then solving the recurrence relation we have

$$P_f[x, s_2 \pm 1] = 1/(3*2^{|x-s_1|-1}) - 1/(2*3^{|x-s_1|}) \quad \text{for } |x-s_1| > 0 \quad \ldots\ldots\ldots\ldots(2.5)$$

$$P_f[s_1 \pm 1, y] = 1/(3*2^{|y-s_2|-1}) - 1/(2*3^{|y-s_2|}) \quad \text{for } |y-s_2| > 0 \quad \ldots\ldots\ldots\ldots(2.6)$$

Case III

For points other than those considered in the above two cases we have the following simple recurrence relation.

$$P_f[x, y] = P_f[x-1, y] * \tfrac{1}{2} + P_f[x, y-1] * \tfrac{1}{2}$$

Now consider the rectangle passing through the point of interest P [x, y] and the source point S as shown dotted in Fig 4.

Consider the vertical and horizontal lines at unit grid distance from the source and nearer to the point P [x, y] in Fig 4.1. The lines RT and RU show these. Now consider any point say R_{h1} on these lines. This point contributes half of its power to the point to its immediate right along RU viz. R_{h2} and the other half to V. So the former half portion is the power that is actually propagated towards the point P. Now after propagating this amount of its power to V, V itself is free to transmit whole of its received power towards P. From V a part of its transmitted power will reach P eventually. This power can reach P through any of the paths from V to P taking the grid lines in between. At each intermediate point in each of these paths the propagation factor reduces by half. Now the number of paths from V to P assuming V is the point $[v_1, v_2]$ is given by

$$\frac{Factorial[(x-v_1)+(y-v_2)]}{Factorial[x-v_1]*Factorial[y-v_2]} = {}^{x+y-(v_1+v_2)}C_{x-v1}$$

where Factorial [a] represents the factorial of the natural number a i.e.
Factorial [a] = 1.2.3...a and ${}^{m}C_n$ is the number of ways of choosing n things out of m ones.

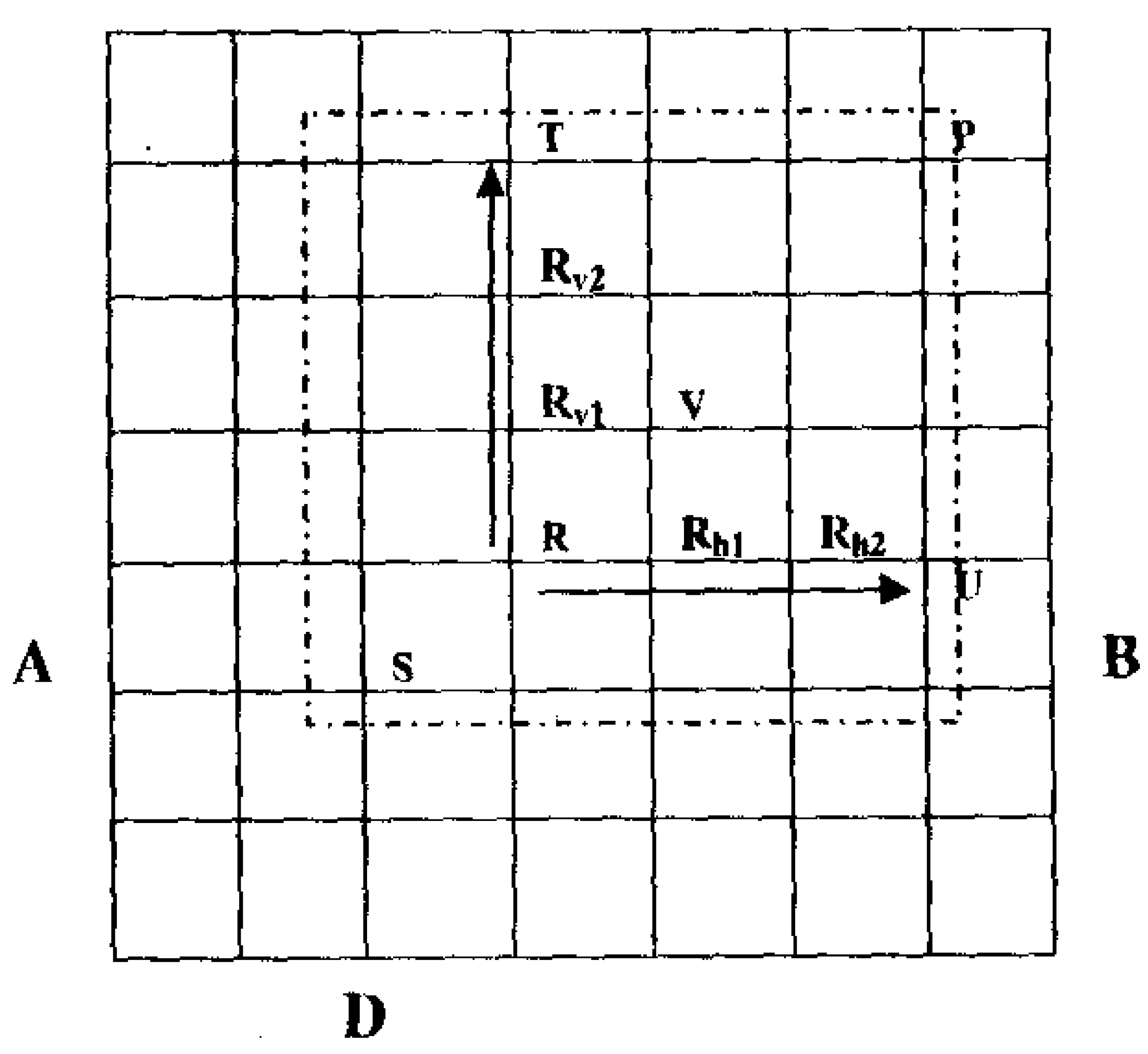

Fig 4.1

Hence the power propagation factor for the power received at point P from V w.r.t V is

$$P_{fvp} = {}^{x+y-(v_1+v_2)}C_{x-v1} * (1/2)^{x+y-(v_1+v_2)} \quad \text{.....................(3.1)}$$

Let P_{fv} be the propagation factor at point V w.r.t source S. Then clearly the actual propagation factor P_f [x, y] at P w.r.t source S will be the summation of $P_{fv} * P_{fvp}$ over all such Vs.

Hence we have,

$$P_f[x, y] = (½)*[\sum_{k=2}^{x} \{1/(3*2^{k-1})-1/(2*3^{k})\} * {}^{x+y-(k+2)}C_{x-k} * (½)^{x+y-(k+2)} +$$

$$\sum_{k=2}^{y} \{1/(3*2^{k-1})-1/(2*3^{k})\} * {}^{x+y-(k+2)}C_{y-k} * (½)^{x+y-(k+2)}] \quad ....(3.2)$$

Hence, the power propagation factors for the three different cases described are given in equations 1.5, 1.6, 2.5, 2.6 and 3.2.